51. IWK

Internationales Wissenschaftliches Kolloquium
International Scientific Colloquium

PROCEEDINGS 11-15 September 2006

FACULTY OF ELECTRICAL ENGINEERING AND INFORMATION SCIENCE

INFORMATION TECHNOLOGY AND ELECTRICAL ENGINEERING - DEVICES AND SYSTEMS, MATERIALS AND TECHNOLOGIES FOR THE FUTURE

Startseite / Index:
http://www.db-thueringen.de/servlets/DocumentServlet?id=12391

TECHNISCHE UNIVERSITÄT
ILMENAU

Impressum

Herausgeber: Der Rektor der Technischen Universität Ilmenau
Univ.-Prof. Dr. rer. nat. habil. Peter Scharff

Redaktion: Referat Marketing und Studentische Angelegenheiten
Andrea Schneider

Fakultät für Elektrotechnik und Informationstechnik
Susanne Jakob
Dipl.-Ing. Helge Drumm

Redaktionsschluss: 07. Juli 2006

Technische Realisierung (CD-Rom-Ausgabe):
Institut für Medientechnik an der TU Ilmenau
Dipl.-Ing. Christian Weigel
Dipl.-Ing. Marco Albrecht
Dipl.-Ing. Helge Drumm

Technische Realisierung (Online-Ausgabe):
Universitätsbibliothek Ilmenau
ilmedia
Postfach 10 05 65
98684 Ilmenau

Verlag:
Verlag ISLE, Betriebsstätte des ISLE e.V.
Werner-von-Siemens-Str. 16
98693 Ilrnenau

ISBN (Druckausgabe): 3-938843-15-2
ISBN (CD-Rom-Ausgabe): 3-938843-16-0

Startseite / Index:
http://www.db-thueringen.de/servlets/DocumentServlet?id=12391

51st Internationales Wissenschaftliches Kolloquium
Technische Universität Ilmenau
September 11 – 15, 2006

A. Jakovics, M. Kirpo, B. Nacke

LES modelling of turbulent structure and mass transfer processes in induction furnaces

ELECTRO-PROCESSING TECHNOLOGIES

Abstract

LES has proved to be a very powerful way to predict velocity dynamics and to resolve large and middle scale turbulent quantities of the flow. It is widely used today for flow calculations in science, engineering and industry. Authors present results of LES modelling of turbulent flows in a induction crucible furnace (ICF) and in a induction furnace with cold crucible (IFCC). Calculated velocity distributions are compared with experimental for Wood's metal (Sn=12.5%, Pb=25.0%, Bi=50% and Cd=12.5%) flow in ICF. Velocity and temperature distributions are calculated for TiAl flow in different IFCC systems. Results represent the large role of turbulent pulsations in IFCC temperature homogenisation. It is shown that LES model can be effectively used for investigation of species transport in the melt using the particle tracing method. The particle tracing was performed for different particle Stokes numbers.

1. Introduction

Electromagnetic heating and melting is one of the most effective methods for conducting material processing and production. The melt flow in induction furnaces and electromagnetic stirrers is formed by Lorentz forces. The flow is turbulent and usually consists of one or several averaged recirculated vortices. The maximal intensities of the flow have characteristic values larger than 1 m/s in industrial equipment. The Lorentz force driven flows studied in this paper consists of the two toroidal averaged flow vortices, which sizes and position depends on geometry and electromagnetic field distribution in the melt. It was established in experiments that measured temperature distribution in ICF is very homogeneous in the whole melt volume. This fact well corresponds to LES modelling results. Temperature gradients in IFCC are even greater, but temperature homogenisation and higher superheat should be obtained for melt alloyage with additions, which can have higher melting temperature. Therefore calculation of average superheat is one of the tasks for computer simulation. From the other side alloyage species transport (for example carbon or silicon), homogenisation or sedimentation are actual problems both for ICF and IFCC, which can substantially influence quality of the final product or lifetime of the installation. Our experience shows

that LES approach together with the particle tracing can be effectively used to solve such problems. The induction melting process is widely used today in industry and research; hence it is a good object for investigation. Computer modelling allows to study parameters of induction equipment before it is built and to improve energy efficiency of melting process. The aim of this work is to study physical parameters of velocity oscillations in the melt flow and to predict velocity and temperature fields in the real induction facilities using LES modelling.

2. Modelling technique

Commercial codes ANSYS and FLUENT were used for electromagnetic field and hydrodynamics calculations respectively. Velocity measurements results in the ICF Wood's metal flow [1], [2] were used for approbation of the LES model in FLUENT.

2.1. Induction crucible furnace model

ICF consists of a cylindrical crucible, which is filled with Wood's metal. Therefore 2D axis-symmetric electromagnetic model was created in ANSYS using current-fed massive conductor approach. Melt shape deformations were not observed in the experiments and therefore free surface oscillations were not taken into account. Produced Lorentz forces were transfered to 3D FLUENT model with characteristic mesh size about 3 mm and specially refined mesh in the side boundary region. Hydrodynamics was calculated using LES model [3] with the 5 ms minimal time step. About 40-60 seconds of the flow development from the rest state were calculated for different model geometries and inductor currents. Central differencies discretization was used for momentum equations and the body force weighted for pressure.

2.2. Induction furnace with cold crucible

IFCC systems are characterized by slitted crucible walls, which are made from copper and intensively cooled with water. Therefore melted material is usually resolidified on the inner crucible walls forming a ”skull”. Melting is provided by the high intensity electromagnetic field, which characteristic power in the whole IFCC facility can exceed 200 kW in the laboratory setup [4]. Therefore melted material usually has curved free surface, which depends on the material amount, EM field frequency and inductor current. 3D EM field model of a one half-slit section was built in ANSYS. This 3D model was used to estimate meniscus shape of the melt. Axial and radial components of the

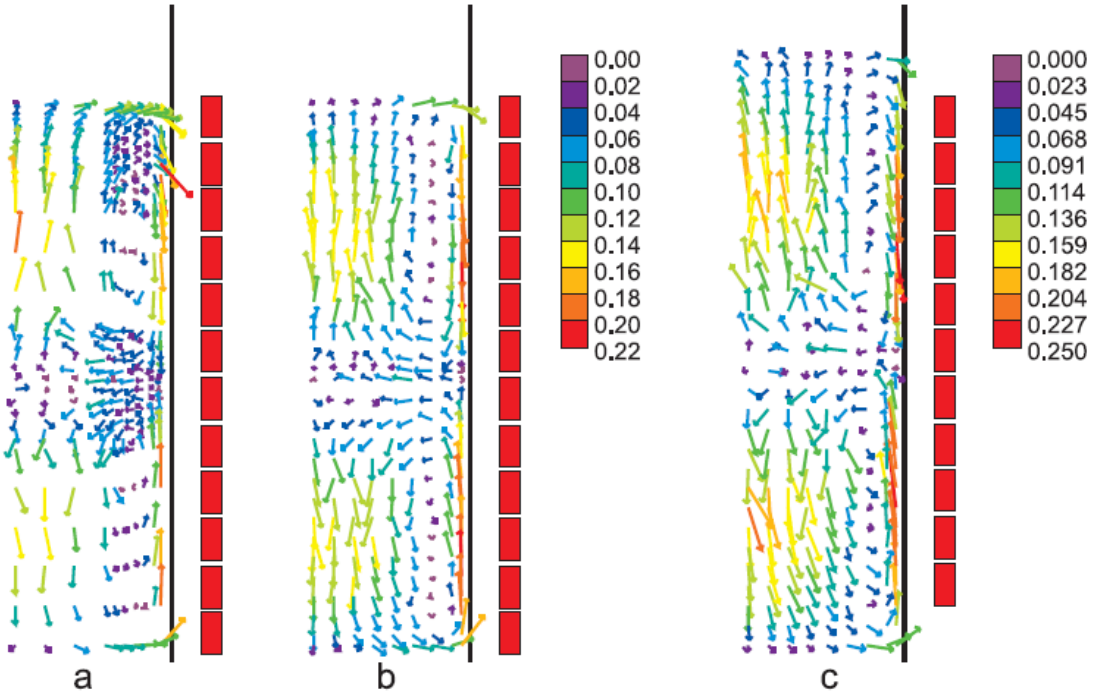

Figure 1: a -experimental old [1], b -experimental 2006 velocity distributions for 57 cm crucible (I=1999 A, f=395 Hz); d -experimental data for 62 cm (I=2180 A). Black line represents crucible wall.

Lorentz force and heat sources were calculated using this 3D EM ANSYS model and transferred to 3D FLUENT model taking into account periodical angular dependence of the above mentioned quantities. Characteristic size of the mesh was below 2 mm and the time step was 5 ms or 10 ms. The Courant number $Cr = \frac{v \cdot \delta t}{\delta x}$, where v is mean velocity, δt and δx are corresponding time step and mesh size was lower than 1 in all cases, so the numerical dispersion does not influence precision of solution. Boundary layers of the model flow regions were refined. No shear boundary conditions were applied to free surfaces and no sleep boundary conditions for walls. For temperature calculations in the IFCC models wall constant temperature and free surface radiation conditions with external emission 0.3 were used.

3. ICF experimental and modelling results and discussion

Several velocity measurement experiments series were made with Wood's metal flow in ICF (melt height 57 or 62 cm, diameter 31.6 cm) with steel crucible in 90-ties [1] and in 2006 (fig. 1). Detailed analysis of experimental data is performed in [1], [5]. Averaged velocity distributions for characteristic flow regimes introduces two main vortices, but in reality instantaneous flow is highly turbulent ($Re>10^4$). Values of radial

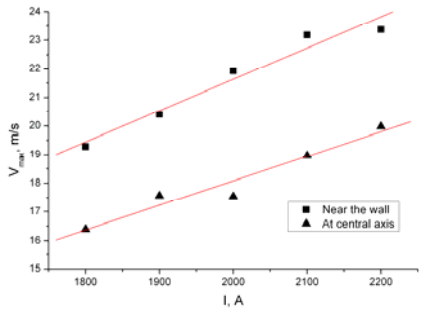

Figure 2: Maximal measured velocity values for H=57 cm melt height and dif ferent inductor currents.

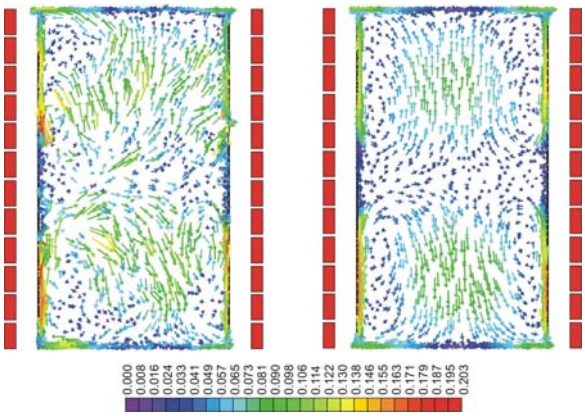

Figure 3: Instantaneous and averaged LES calculated velocity distributions (I=1990 A).

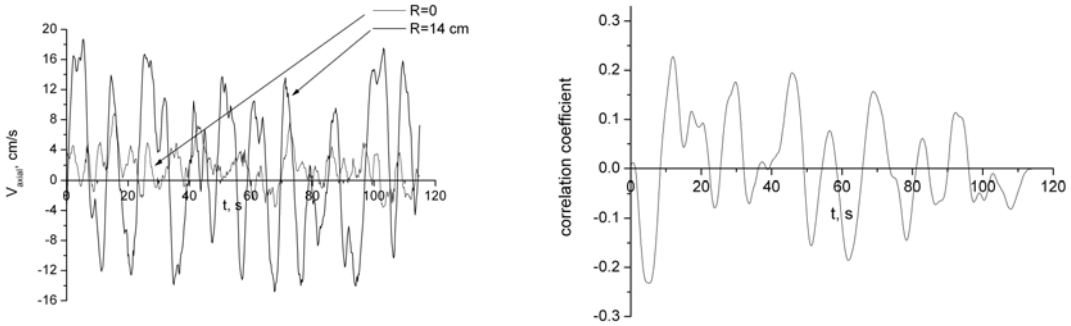

Figure 4: Measured axial velocity low-frequency oscillations between the vortexes (left) and corresponding 2 point correlation (right).

and axial velocity components of the flow were measured by a permanent magnet sensor [6] (scanning rate about 20 Hz) for 60 seconds in every point of discrete grid. Electromagnetic field with a frequency ranged from 300 to 1500 Hz was generated by a 12-coil inductor (current from 1000 A to 2200 A). A constant crucible temperature of about 80^{o}C was kept to avoid temperature fluctuations influence on the flow. In this case melt temperature in the crucible was about 115^{o}C. In most of the experiments the filling level was equal to the inductor height (100%). Two different ICF geometries were tested in the last experiments. The first corresponds to the 57 cm melt height, 2000 A current and 12 turn inductor, which height equals to melt height. In the second case one inductor turn from the bottom was disconnected, melt height was increased to 62 cm and current was increased to 2180 A to provide the same power in the melt. For data acquisition digital DELPHIN unit with 24 bit ADC was used.

Characteristic flow velocities can be taken on the symmetry axis and near the wall at approximately half height of the averaged vortex. As it should be maximal velocities have linear dependence on current *v*~I (figure 2). The averaged vortex centres are

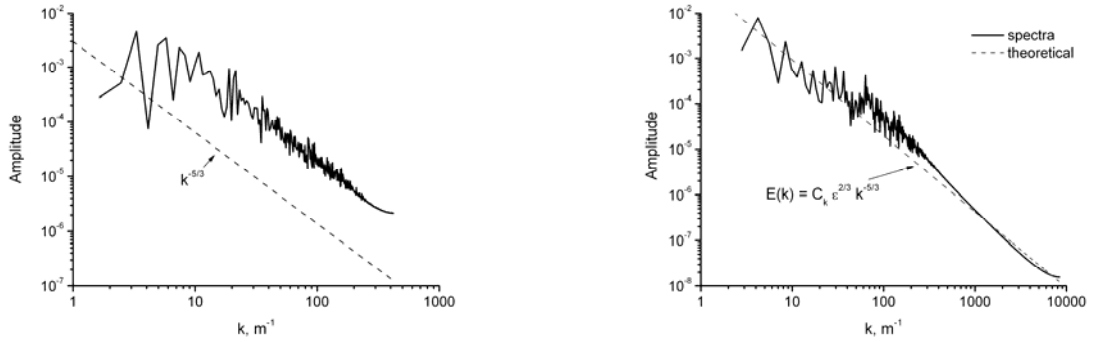

Figure 5. Experimental (left) and calculated (right) turbulent energy spectra at symmetry axis.

shifted closer to the wall and are placed at distance 3/4 of the radii. Therefore velocities near the wall are higher because mass conservation law. LES calculated characteristic velocity distributions in selected time moment and averaged over 50 seconds represents flow structure (figure 3), which is close to seen in experiments.

The structure of two-point measured axial velocities is near periodic (figure 4 left). Low-frequency oscillation amplitude near the wall between the vortices is large and can achieve at least the half of the maximal flow velocity. It can be explained with high intensities of the vortices near the wall. In the centre of the melt flow oscillation amplitude is 3-4 times lower. Velocity correlation coefficients $B_{ii}(\Delta\vec{r}) = \overline{v_i(\vec{r},t)v_i(\vec{r}+\Delta\vec{r},t)}$ were computed (figure 4 right). The local $B_{ii}(\Delta\vec{r})$ maximums at t≈12-15 s correspond to low frequency oscillation period, while the circumference period of the fluid element in the averaged toroidal vortex is about 25-30 s. Taking inverse Fourier transform from autocorrelation coefficients $R_{ii}(\tau) = \overline{v_i(\vec{r},t)v_i(\vec{r},t+\tau)}$ the Eulerian time spectrum can be produced [7]. Full energy spectra was computed adding three component spectrums together using isotropic turbulence approximation and then converted into wave number spectra using Taylor's hypothesis: $k = \omega/v$, where $v \approx 0.09$ m/s is averaged velocity at current point (figure 5). It can be shown that smaller scales of turbulent structures, which can be distinguished in our LES model is about 0.6 cm [2].

All spectra have several frequencies with relatively high energy (this effect can be best noticed on figure 5 (left)). Maximal wavenumber with high energy in experimental spectra is about 20 m^{-1}. Corresponding vortex size is 5 cm. Computed and experimental spectra can be compared with the theoretical Kolmogorov spectrum in the inertial subrange [7]:

$$E(k) = C_k \varepsilon^{2/3} k^{-5/3}, \ \varepsilon = 2\nu \int_0^{+\infty} k^2 E(k) dk \qquad (1)$$

where ε is turbulent dissipation rate computed from the energy spectrum, ν =4.5·10^{-7} m^2/s and Ck =1.5 for the melt. Dashed lines on figure 5 (right) represents theoretical curves calculated by these formulas. The inertial range is narrow because our mesh and selected time step restrict observation of high scale oscillations. Decay of computational curve at high k values is more rapid because subgrid viscosity and numerical effects.

Our calculations technique make possible anisotropy analysis of the flow. Flow anisotropy can be studied in different ways using different reference values. We have selected coefficients $G_{ij,kl}$ as anisotropy measure [8]:

$$G_{ij,kl} = \frac{\langle (\partial u_j / \partial x_i)^2 \rangle}{\langle (\partial u_l / \partial x_k)^2 \rangle}, i, j, k, l = x, y, z \qquad (2)$$

Calculations should be performed with fluctuations (averages are removed) [9] for correct analysis. We have selected point at the centre of the crucible (on symmetry axis between upper and lower averaged vortices) where average velocity is zero and anisotropy analysis can be made directly on velocity gradients. Example values are represented in table 1, where they can be compared with theoretical values for isotropic turbulence [8]. As it can be seen recirculated flow in the crucible has turbulence anisotropy. Coefficient values in other parts of the flow are even larger, so we can conclude that isotropic laws can not be applied for such types of the flows.

Point	*Gxx,yx*	*Gxx,zx*	*Gxy,yy*	*Gxz,zz*	*Gxy,zy*	*Gxz,yz*
Isotropic [8]	0.5	0.5	2	2	1	1
r=0, z=0	6.4	24.9	1.2	1.5	4.7	1.2

Table 1: Relative strength of velocity gradients in different directions.

Particle tracing can be additionally performed using LES model. Motion of the particles was determined by integrating the force balance in a Lagrangian reference frame:

$$\frac{\mathrm{d}\vec{u}_p}{\mathrm{d}t} = \vec{F}_D(\vec{u} - \vec{u}_p) + \vec{g}\frac{\rho_p - \rho}{\rho_p} + \vec{F}, \qquad (3)$$

where $\vec{u}$ is the melt phase velocity, $\vec{u}_p$ is the particle velocity, ρ is the melt density, ρ_p is the particle density, $\vec{F}$ is the possible additional acceleration and $\vec{F}_D(\vec{u} - \vec{u}_p)$ is the drag force per unit particle mass. F_D can be expressed as:

$$F_D = \frac{18\mu}{\rho_p d_p^2}\frac{C_D \mathrm{Re}}{24}, \quad \mathrm{Re} = \frac{\rho d_p |\vec{u}_p - \vec{u}|}{\mu}. \qquad (4)$$

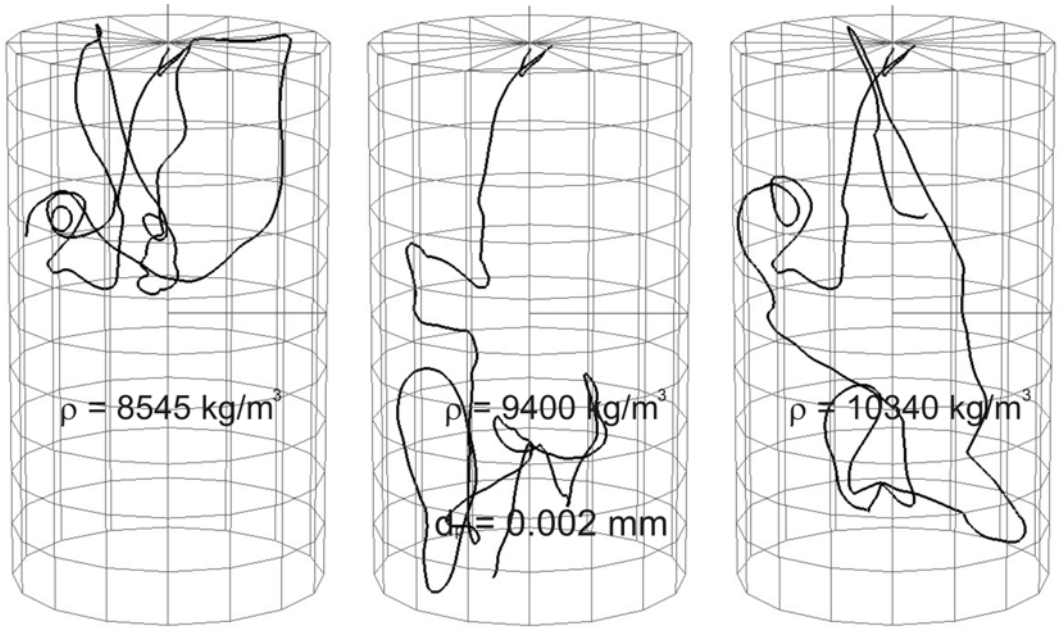

Figure 6: Particles injected from the top, gravitation is on, d_p=0.002 mm.

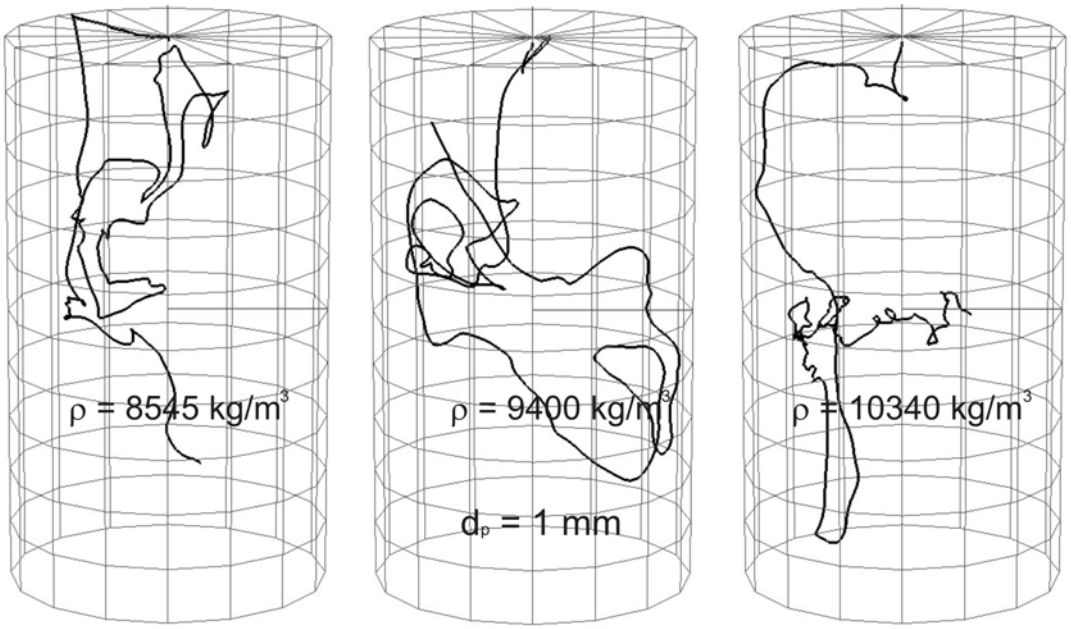

Figure 7: Particles injected from the top, gravitation is on, d_p=1 mm.

These formulas include μ, which is the molecular viscosity of the melt, and d_p, which is the particle diameter. C_D is the drag coefficient and for spherical particles it can be taken from [10]. Additional acceleration $\vec{F}$ was selected to be zero, but it can include EM separation force or Saffman lift force if necessary. We have also made several assumptions:

- particle-particle interaction is negligible,
- all particles are rigid spheres,
- particles do not affect the structure and velocities of the flow.

The motion of particles can be described with dimensionless parameter, which is called Stokes number: $\mathrm{St} = \tau_p / \tau_\eta$, where the dissipation time τ_η is essentially the overturn time of Kolmogorov's eddy of size η ($\tau_\eta = \sqrt{\nu/\varepsilon}$) and τ_p is the particle fluid response time. Particles become more fluid-like as St approaches zero and are distributed more uniformly in an incompressible fluid flow. When St exceeds unity, particles become less responsive to the flow field, behaving more like random walkers, and as such are also distributed more uniformly. The most nonuniform distributions result when St is at or near unity [11]. The Stokes number can also be expressed as [12]:

$$\mathrm{St} = \frac{\rho_p d_p^2 U_0}{18 \mu L_0}, \qquad (5)$$

where U_0=0.1 m/s and L_0=0.16 m are characteristic flow velocity and length scale. The maximal Stokes number of particles injected to Wood's metal is about 0.4. Therefore all particles are strongly affected by the melt vortices. As it was shown before [2], absence of gravity makes all particles to drift inside the melt and particle separation is determined by F_D, witch is proportional to ρ/ρ_p ratio (4). If gravitation is switched on, then the particle trajectories are strongly affected by $\vec{g}$. If the difference between particle density and fluid density is large then particle can be drown ($\rho_p>\rho$) or rise to the surface ($\rho_p<\rho$). Then according to flow direction particle goes to the wall and oscillates there in angular direction (figure 9 right). If density ratio ρ/ρ_p is about 1.1 then gravitation role in particle decomposition is decreased and particles again are distributed inside the melt, but this effect depends on the particle size and density. For small particle size (d_p=0.002 mm (figure 6) and respectively small Stokes numbers density role is neglected. Both "light" and "heavy" particles can be entrapped in the upper part of the flow. Particle tracks show good reaction to the

melt flow.If d_p is larger then density role increases. If (ρp >ρ then the particle can be entrapped in the near wall region (figure 7 right). This is noticed mainly for particles with d_p=1 mm and is repeated in several computational runs. Comparing averaged particle velocities one can say, that entrapped particle has the lowest average velocity, which can be 30% less than average velocity of the flow. Particle injection depends on particle size too. ”Heavy” 1mm particle is affected by the flow closer to the crucible bottom. The distance, when particles of equal sizes are separated depends on Stokes number. For small St particles can go together for a relatively long time (for 0.002 mm this time is larger than 5 s). For large St all particles are separated immediately. The particle with ρ_p=ρ goes together with the flow while particles with other densities are separated from the flow and goes together longer distance.

4. Cold Crucible furnace parameter study

CCF calculations were performed with parameters described in table 2. Both k-

TiAl m, kg	Melt r, cm	Melt h, cm	I, kA	F, kHz	P_{melt} kW	k-ε V_m, m/s	k-ε T_m, K	LES V_m, m/s	LES T_m, K	ANSYS model
6	6	20.1	4.8	8.5	53.5	0.9		1.20	1791	2D
6	7	16.8	4.8	8.5	53.5	1.11		1.55	1790	2D
6	8	13.5	4.8	8.5	53.5	1.48		1.46	1791	2D
7	8	15.3	6.5	5	36.3	1.41	1791	1.33	1795	3D
7	8	13.1	5	10	38.5	1.16	1796	1.16	1800	3D
7	8	11.9	4	20	44.5	1.11	1801	1.14	1807	3D

Table 2: CCF parameter study (maximal velocities and temperatures, current amplitude).

ε and LES models were used for every case. First three cases were calculated without azimuthal dependence of Lorentz force distribution (2D EM ANSYS model). Other cases included angular force dependence because 3D ANSYS electromagnetic model was used. LES predicted temperature distribution in the TiAl melt is very homogeneous and overheat is higher then in k-ε model if angular dependence of induced heat is taken into account. Averaged LES and k-ε velocity results are comparable in all cases except those with smaller crucible radius.

Analysis show that maximal overheat temperature in the melt is higher when the frequency is higher. For 5 kHz field and 6500 A current overheat temperature is about 22 K, but for 20 kHz it is about 34 K, which is at least 30% higher. The Joule heat induced in the melt is 6 kW larger at 20 kHz, but the full system power is 30% less than

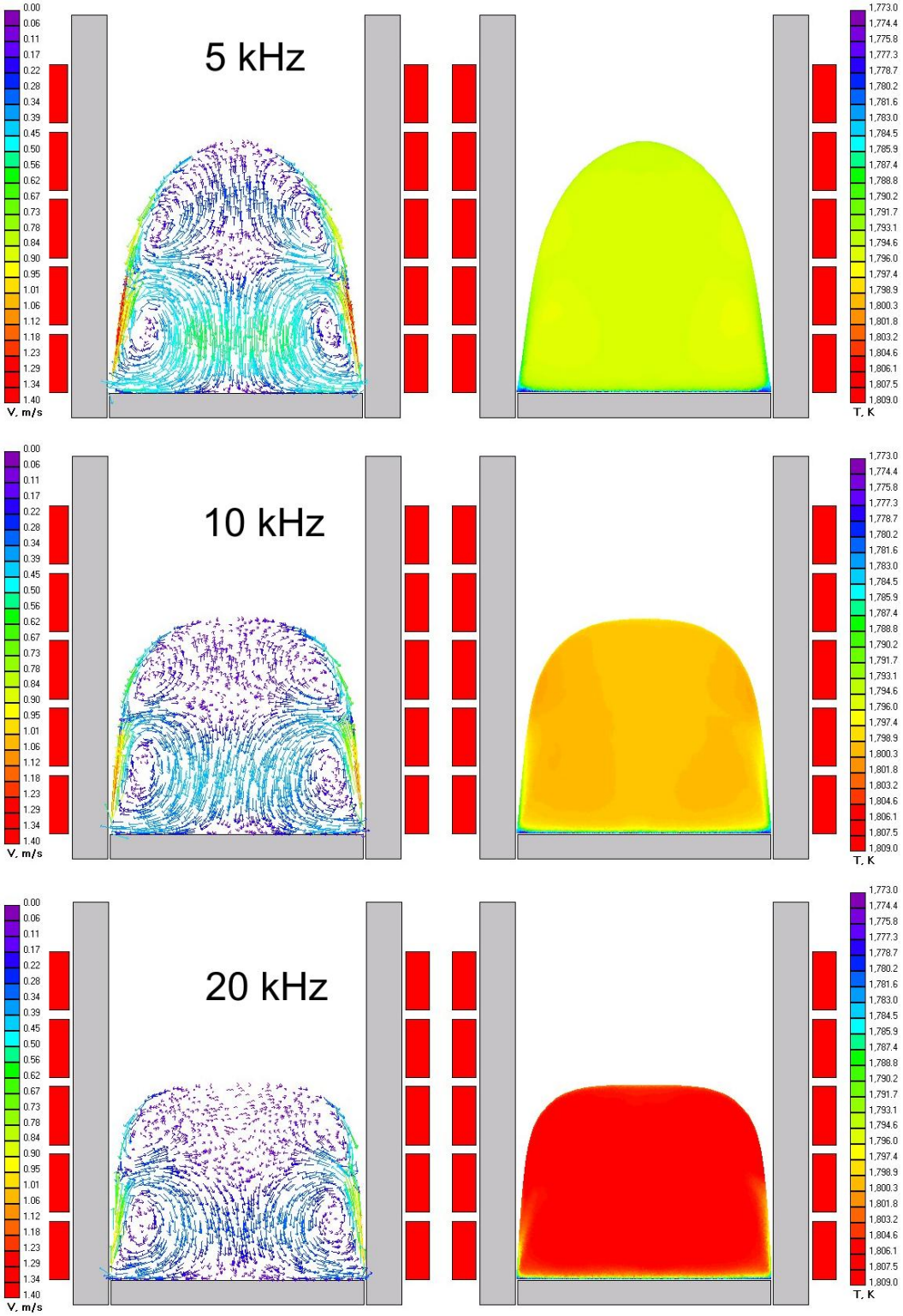

Figure 8: Velocity and temperature distributions for 7 kg TiAl, F=10 kHz, P_{melt}=38.5 kW.

at 5 kHz. Maximal velocities in the flow are observed in the lower vortex in the near surface region (figure 8). Maximal velocity values decreases when EM field frequency becomes larger. Comparing values calculated by k-ε and LES models one can say that maximal velocity values are approximately the same, but LES calculated maximal temperatures are higher and we think closer to the real values. It means that LES more correctly describes heat transfer processes inside the melt.

Particle tracing was performed together with LES modelling. For 10 kHz IFCC model two particle triplets were put inside the melt at t=0 (after obtained k-ε solution) and about 16 s of the flow were computed with 0.002 ms time step. Boundary conditions were set to reflection on all surfaces. The first triplet was dropped 1 cm from the meniscus top and the second one was dropped 1 cm from the bottom on symmetry axis (figure 9). Densities of the particles were selected to be 375, 3750 (density of TiAl melt) and 37500 kg/m^3. As it is shown, the heaviest particle with St≈15 all the time is placed in the lower corner of the melt. But even there it still oscillates in tangential direction and during these oscillations can draw a circle (figure 9 bottom right). Light particle tries to go

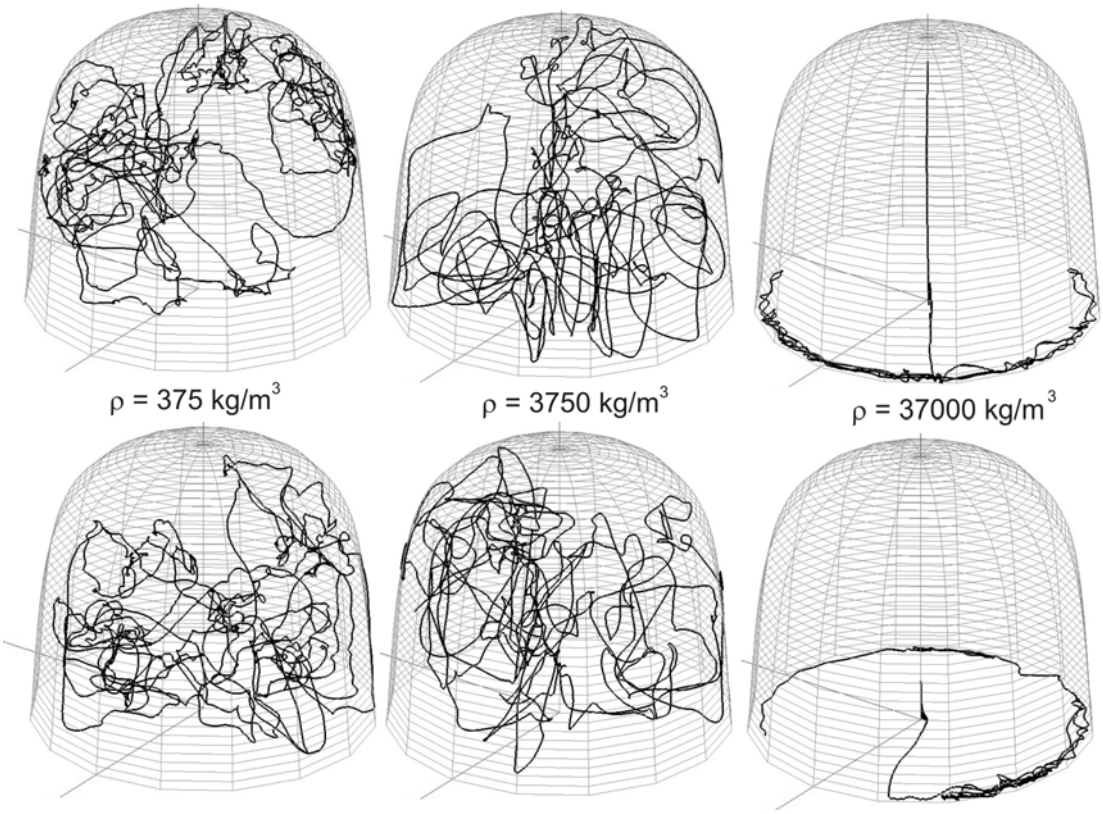

Figure 9: IFCC unsteady LES particle tracing, particles released from top (above) and from bottom (below)

to the surface and then is involved inside the melt due to the presence of the curvature in the meniscus shape. Under the top surface of the melt there is a strong melt flow (0.3-0.4 m/s) downwards, which easily catches light particle and brings it down into the vortex interaction zone. So in case of high intensity flows in IFCC the particles with densities lower or equal to the melt density can not be trapped on the surface of the melt. The trajectory of light particles and TiAl density particles are approximately the same.

Stokes numbers computed using expression (5) cover range from 0.16 to 15.63. For Stokes number calculations characteristic velocity value was U_0=0.33 m/s and characteristic distance was L_0=4 cm. Average velocity of the particles inside the melt is about 0.33 m/s, but for the particles with the large density this value is smaller because such particles are intrepped in the bottom conner, where flow intensity is less.

5. Conclusions

Experiments in the ICF filled with Wood's metal were made with different inductor currents and metal filling levels. The patterns of averaged flow and two point measurements of the axial velocity components are obtained. Performed LES computer simulation have the same characteristics (characteristic velocity values and vortex structure) as the measured mean flow. Wavenumber space experimental and computational spectrums are in accordance with the Kolmogorov's theory. LES calculated temperature distribution in IFCC does not have large temperature gradients. Angular dependence of Lorentz force distribution and Joule heat sources increases computed average temperature of the melt in IFCC. Particle tracing shows high intensity of the convective transfer mechanism in both IFC and IFCC.

Acknowledgements

Part of this work was carried out with the IBM pSeries Supercomputer of the HLRN and the authors thank all members from the HLRN for their support. Also this work has been supported by the European Social Fund (ESF).

References:

[1] E. Baake. Grenzleistungs- und Aufkohlungsverhalten von Induktions-Tiegelöfen, VDI, Düsseldorf, 1994.

[2] M. Kirpo, A. Jakovics, E. Baake, B. Nacke. Analysis of Experimental and Simulation Data for Liquid Metal Flow in a Cylindrical Container. In *Modelling for Material Processing*, pp. 36–41, Riga, 2006.

[3] P. Sagaut. *Large Eddy Simulation for Incompressible Flows, 2nd edition.* (Springer, 2002.)
[4] V. Bojarevics, R. A. Harding, K. Pericleous, and M. Wickins. The development and experimental validation of a numerical model of an induction skull melting furnace. *Metallurgical and materials transactions B*, vol. 35B (august 2004), pp. 785–803.
[5] M. Kirpo, A. Jakovics, E. Baake. Characteristics of velocity pulsations in turbulent recirculated melt flow. *Magnetohydrodynamics*, vol. 41 (2005), pp. 199–210.
[6] R. Ricou and C. Vives. Local velocity and mass transfer measurements in molten metals using an incorporated magnet probe. *Int J Heat Mass Transfer* vol. 25 (1982), pp. 1579– 1588.
[7] H. Tennekes, J.L. Lumley. *A First Course in Turbulence.* (The MIT Press, London, 1972.)
[8] B.S. Pope. *Turbulent flows.* (Cambridge University Press, 2005.)
[9] William D. Smyth and James N. Moum Anisotropy of turbulence in stably stratified mixing layers *Phys. Fluids.*, vol. 12 (June 2000), Issue 6, pp. 1343–1362.
[10] S. A. Morsi and A. J. Alexander. An Investigation of Particle Trajectories in Two-Phase Flow Systems.*J. Fluid Mech.*, 55(2) (1972), pp. 193–208.
[11] R. Hogan and J. Cuzzi. Stokes and Reynolds number dependence of preferential particleconcentration in simulated three-dimensional turbulence. *Phys. of Fluids.*, vol. 13, num. 10, pp. 2938–2945.
[12] K. Luo, J. Fan, H. Jin and K. Cen. LES of the turbulent coherent structures and particle dispersion in the gas-solid wake flows. *Powder Technology.*, 147 (2004), pp. 49–58

Authors:

Prof. Dr.-Phys. Andris Jakovics
Dipl.-Phys. Maksims Kirpo
Laboratory for Mathematical Modeling of Environmental and Technological Processes, University of Latvia, Zellu str. 8
LV-1002 Riga, Latvia
Phone: +371 7033780
Fax: +371 7033781
E-mail: ajakov@latnet.lv

Prof. Dr.-Ing. Bernard Nacke
Institute for Electrothermal Processes, University of Hanover, Wilhelm-Busch-Str. 4
D-30167 Hanover, Germany
Phone: +49 511 762 3248
Fax: +49 511 762 3275
E-mail: nacke@ewh.uni-hannover.de